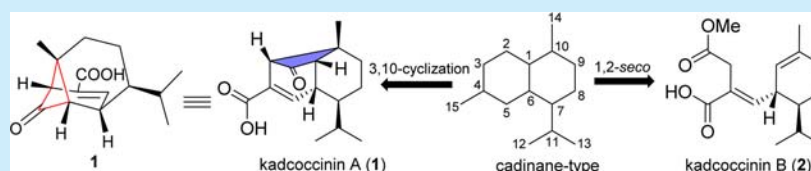


Structural Characterization of Kadcoccinin A: A Sesquiterpenoid with a Tricyclo[4.4.0.0^{3,10}]decane Scaffold from *Kadsura coccinea*Zheng-Xi Hu,^{†,‡,§} Yi-Ming Shi,^{†,§} Wei-Guang Wang,[†] Jian-Wei Tang,[†] Min Zhou,[†] Xue Du,[†] Yong-Hui Zhang,^{*,‡} Jian-Xin Pu,^{*,†} and Han-Dong Sun[†][†]State Key Laboratory of Phytochemistry and Plant Resources in West China, Kunming Institute of Botany, Chinese Academy of Sciences, Kunming 650201, China[‡]Hubei Key Laboratory of Natural Medicinal Chemistry and Resource Evaluation, School of Pharmacy, Tongji Medical College, Huazhong University of Science and Technology, Wuhan 430030, China

S Supporting Information



ABSTRACT: Kadcoccinin A (1), a cage-like sesquiterpenoid possessing a tricyclo[4.4.0.0^{3,10}]decane scaffold, and the biosynthetically related kadcoccinin B (2) were isolated from the stems of *Kadsura coccinea*. Their structures and absolute configurations were determined from extensive spectroscopic analysis and quantum chemical calculations. Additionally, their cytotoxic and antifungal effects were initially evaluated, and a plausible biosynthetic pathway was proposed.

Recently, the Schisandraceae family, which is subdivided into two genera, *Schisandra* and *Kadsura*, has been a hot research topic not only because of the numerous pharmaceutical advantages,¹ such as antitumor activity,² anti-HIV-1 activity,³ antifeedant effect,^{3b} antiplatelet aggregation activity,⁴ and protective activity against H₂O₂-induced oxidative damage on Caco-2 cells,⁵ but also because of the huge challenges associated with synthesizing the Schisandraceae triterpenoids characterized by the intricate ring systems and multiple chiral centers.⁶

Previously, we reported six new lanostane-related triterpenoids possessing diverse skeletons from the stems of *Kadsura coccinea* collected from the region of the Menglun, Yunnan Province, People's Republic of China.⁷ As a part of our ongoing program to discover more structurally intriguing and bioactive natural products, we performed a chemical investigation on the ethyl acetate extract to afford kadcoccinin A (1) bearing a tricyclo[4.4.0.0^{3,10}]decane scaffold, along with a rare cadinane-related sesquiterpenoid, kadcoccinin B (2) (Figure 1). Interestingly, 1 featured a special bicyclo[3.1.1]heptane moiety, in which a cyclobutane unit gives rise to a large, long-range spin–spin coupling (⁴J_{1,3} ≈ 7.0 Hz) between the bridge-head protons. To our knowledge, a long-range coupling between two protons

distributed in a W correlation in a bicyclo ring system is an intriguing phenomenon reported in typical cases.⁸ Because of the cage-like architecture and deceptive NMR data of 1, quantum chemical calculations were used to verify the final structure and absolute configuration. This paper elaborates on the isolation, structural characterization, biological activities, and postulated biogenetic pathway of 1 and 2.

Kadcoccinin A (1) was determined to be C₁₅H₂₀O₃ from an HRESIMS at *m/z* 247.1341 ([M – H][–], calculated as 247.1340). The IR spectrum displayed absorptions that were attributed to carboxyl (1778 cm^{–1}), ketone (1690 cm^{–1}), and olefinic double bond (1632 cm^{–1}) functionalities. The ¹H NMR spectrum (Table 1) of 1 showed signals for one singlet methyl at δ_H 1.26 (H₃-14), two doublet methyls at δ_H 0.88 (d, *J* = 6.6 Hz, H₃-12) and 0.90 (d, *J* = 6.6 Hz, H₃-13), and one olefinic proton at δ_H 6.81 (br s, H-5). The ¹³C NMR and DEPT spectra (Table 1) revealed 15 carbon signals that were assigned to three methyls, two methylenes, six methines (one olefinic), and four quaternary carbons (two carbonyl and one olefinic). The molecular formula required six indices of hydrogen deficiency, but only one ketone at δ_C 203.1 (C-2), one carboxyl at δ_C 169.9 (C-15), and two olefinic carbons resonating at δ_C 132.2 (C-4) and 145.3 (C-5) were detected, illustrating that 1 had a tricyclic structure.²

Despite the fact that both H-5 and H-6 appeared to be broad singlets with no recognizable vicinal coupling signals, the obvious ¹H–¹H COSY cross-peaks of H-5/H-6/H-1 established the presence of the –C1–C6–C5– subunit. Additionally, the

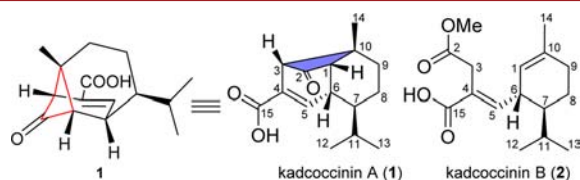


Figure 1. Structures of compounds 1 and 2.

Received: March 31, 2016

Published: April 19, 2016

Table 1. ^1H and ^{13}C NMR Spectroscopic Data for Compound **1** and Its Calculated ^{13}C NMR Data (δ in ppm, J in Hz)

no.	δ_{H}	δ_{C}		
	exptl ^a	exptl ^b	exptl ^c	calcd ^d
1	2.52 dd (3.9, 6.7)	61.2 CH	61.8	62.8
2	—	203.1 C	203.5	203.0
3	3.55 d (6.7)	62.8 CH	64.3	65.3
4	—	132.2 C	134.6	130.0
5	6.81 br s	145.3 CH	142.8	147.6
6	3.02 br s	42.9 CH	43.3	47.3
7	1.37 m	44.1 CH	44.5	47.0
8	0.9 overlapped; 1.69 m	23.8 CH ₂	24.4	25.7
9	1.44 m; 1.67 m	25.1 CH ₂	25.4	27.1
10	—	32.1 C	32.4	36.9
11	1.45 m	32.1 CH	32.4	35.8
12	0.88 d (6.6)	20.1 CH ₃	20.4	19.0
13	0.90 d (6.6)	20.5 CH ₃	20.8	21.3
14	1.26 s	25.2 CH ₃	25.5	24.5
15	—	169.9 C	168.5	163.6

^aRecorded in CDCl_3 at 600 MHz. ^bRecorded in CDCl_3 at 150 MHz.

^cRecorded in $\text{C}_5\text{D}_5\text{N}$ at 150 MHz. ^dCalculated ^{13}C NMR data of **1** in CDCl_3 .

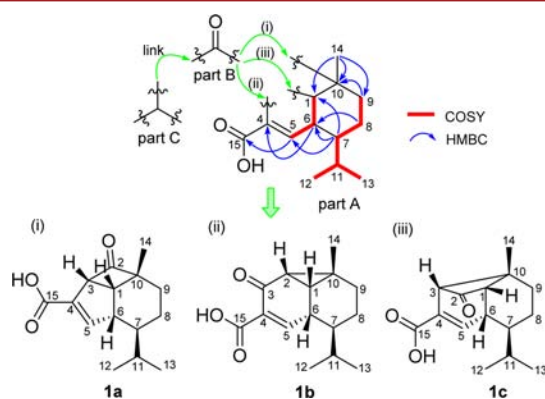


Figure 2. Structural characterization of **1** based on its NMR spectra data and the corresponding three possible structures.

^1H – ^1H COSY correlations of H-12/H-11, H-13/H-11, and H-11/H-7/H-8/H-9, coupled with the HMBC correlations of H₃-14 with C-1, C-9, and C-10; H-9 with C-10; H-8 with C-6; H-7 with C-1, C-5, and C-6; H-6 with C-4; and H-5 with C-15, ascertained the planar structure of subunit part A (Figure 2).

Based on the molecular formula of compound **1**, we were uncertain regarding how the remaining two partial subunits (parts B and C) constructed the tricyclic framework, and three possible structures (**1a**, **1b**, and **1c**) were proposed (Figure 2). First, a strong ^1H – ^1H COSY correlation between the two methines (δ_{H} 3.55 and 2.52) indicated that part C might be linked to C-1, thus, a –CH–CH(1)– unit existed, and the corresponding structures **1a** and **1b** were constructed.

In structure **1a** (Figure 3), the HMBC correlations of H-3 with C-4, C-5, and C-15 seemed to clearly indicate that the planar structure was correct. However, the apparent four-bond HMBC correlations from H-9 and H₃-14 to C-3 puzzled us.⁴

The nuclear Overhauser effect (NOE) is normally recognized as one of the most effective approaches for structural characterization and conformational analysis. However, when the internuclear distance was less than 3 Å, the NOE correlations could be observed even when the two spin systems were in

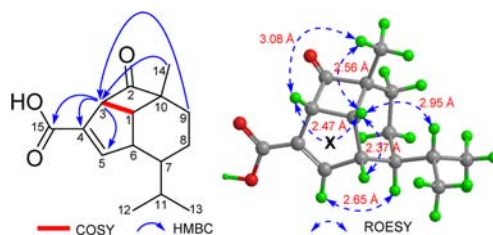


Figure 3. Selected ^1H – ^1H COSY, HMBC, and ROESY correlations of **1a**.

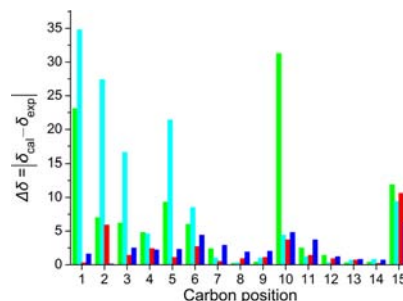


Figure 4. Comparison of calculated ^{13}C chemical shifts for three possible structures, **1a** (green), **1b** (cyan), and **1c** [red, at the B3LYP/6-31++G(2d,2p) level; blue, at the MPW1PW91/6-31G(d,p) level], with experimentally observed shifts.

opposite directions. First, H-1 was randomly assigned to be β -oriented (Figure 3), and the distances of H-3 β /H₃-14 β and H-3 β /H-1 β were 3.08 and 2.47 Å, respectively. However, the obvious ROESY correlation of H-3 β /H₃-14 β and no correlation of H-3 β /H-1 β did not support the above-mentioned results even if the other ROESY correlations (recorded in $\text{C}_5\text{D}_5\text{N}$) were compatible. Hence, we had to review the accuracy of the structure. To further verify the structure, a calculation of the ^{13}C NMR chemical shifts of structure **1a** from the density-functional theory (DFT) calculation at the MPW1PW91/6-31G(d,p) level with the PCM in CDCl_3 was performed. Particularly, the calculated chemical shifts in the cyclobutane motif introduced more errors compared to those in the experimental data, with deviations of 23.1 ppm for C-1 and 31.3 ppm for C-10 (Figure 4). The correlation coefficient (R^2) was 0.9645, and the mean absolute error (MAE) and the corrected mean absolute error (CMAE) were 7.1 and 7.3 ppm (Figure 5A; Table S4), respectively. Accordingly, it did not suggest that structure **1a** was the right one.

In structure **1b** (Figure 6), the HMBC correlations of H-9 and H₃-14 with C-2; H-1 with C-3; and H-2 with C-4 also seemed to support the structure. However, the obvious four-bond HMBC correlations of H-2 with C-5 and C-15 made us doubtful again. After careful analysis of the ROESY spectrum (recorded in $\text{C}_5\text{D}_5\text{N}$), we could not find direct evidence to prove the fault of the structure because of the clear ROESY correlations of H-2/H₃-14, H₃-14/H-1/H-6, H-5/H-7, and H-1/H-11, and no correlation of H-1/H-2 was observed despite a distance of 2.58 Å. Thus, it became more difficult to draw any convincing conclusions based on this data, so it was necessary to perform a calculation of the ^{13}C NMR chemical shifts at the MPW1PW91/6-31G(d,p) level with the PCM in CDCl_3 . The calculated chemical shifts at C-1, C-2, C-3, and C-5 showed large errors compared to those in the experimental data, and the corresponding deviations were 34.8, 27.4, 16.6, and 21.4 ppm (Figure 4), respectively. The correlation coefficient (R_2) was

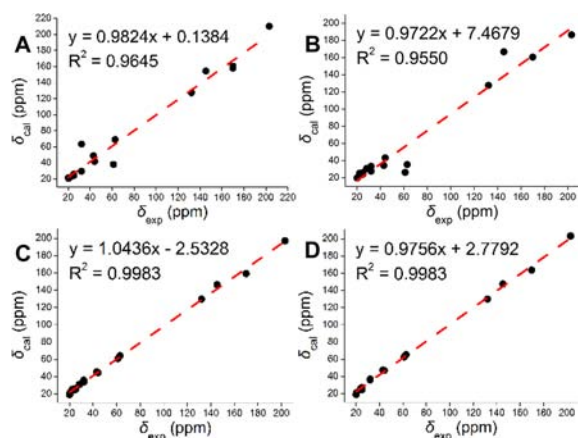


Figure 5. Regression analysis of experimental versus calculated ^{13}C NMR chemical shifts of **1a** [A, at the MPW1PW91/6-31G(d,p) level], **1b** [B, at the MPW1PW91/6-31G(d,p) level], and **1c** [C and D, at the B3LYP/6-31++G(2d,2p) and MPW1PW91/6-31G(d,p) levels, respectively]; linear fitting was shown as a line.

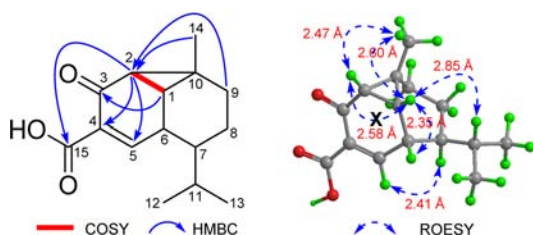


Figure 6. Selected ^1H – ^1H COSY, HMBC, and ROESY correlations of **1b**.

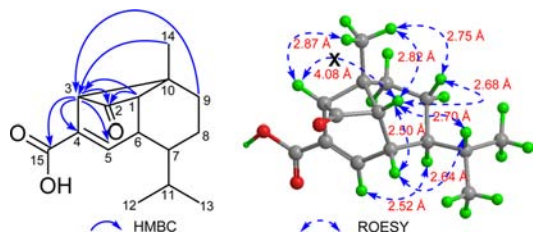


Figure 7. Selected HMBC and ROESY correlations of **1c**.

0.9550, and the MAE and CMAE data were 8.8 and 14.0 ppm (Figure 5B; Table S4), respectively, indicating that structure **1b** was not suitable either.

Because structures **1a** and **1b** were unreliable, we considered **1c**, which contained a bicyclo[3.1.1]heptane moiety and a special long-range spin–spin coupling of H-1/H-3 ($^4J_{1,3} \approx 7.0$ Hz) that subsequently occurred in the cyclobutane unit. In structure **1c** (Figure 7), including the corresponding ^1H – ^1H COSY and HMBC correlations of the subunit part A as mentioned above, the additional HMBC correlations of H-9 and H₃-14 with C-3; H-1 with C-2 and C-3; and H-3 with C-2, C-4, C-5, and C-15 fully ascertained the planar structure of **1c**.

The relative configuration of structure **1c** was determined by the 600 MHz ROESY spectrum in $\text{C}_5\text{D}_5\text{N}$ (Figure 7). By randomly assigning H-1 to be β -oriented, the key ROESY cross-peaks of H-3/H₃-14/H-1/H-6/H-11 revealed that H-1, H-3, H-6, and H₃-14 were cofacial and β -directional, and H-7 should be α -oriented. In addition, the C-4/C-5 olefin of structure **1c** had *E*-geometry based on a key ROESY correlation between H-5 and H-7. Remarkably, the distance between H-1 and H-3 was 4.08 Å,

which corresponds to there being no H-1/H-3 correlation in the ROESY spectrum. Consequently, the relative configuration of structure **1c** was established.

The predominant conformer (39%, Figure 7) was generated at the B3LYP/6-31G(d) level, supporting the above-mentioned results. To further verify the structure, a calculation of the ^{13}C NMR chemical shifts of structure **1c** at the B3LYP/6-31++G(2d,2p) (Figure 5C) and MPW1PW91/6-31G(d,p) (Figure 5D) levels with the PCM in CDCl_3 was obtained, and the calculated chemical shifts agreed well with the experimental data, of which the B3LYP/6-31++G(2d,2p) method showed a correlation coefficient (R_2) of 0.9983, and the MAE and CMAE data were 2.3 and 3.8 ppm (Table S5) respectively. The MPW1PW91/6-31G(d,p) method showed a correlation coefficient (R_2) of 0.9983, and the MAE and CMAE data were 2.5 and 3.8 ppm (Table S5) respectively, indicating that structure **1c** was the most suitable. Overall, the structure and relative configuration of **1** were established to be the same as those for structure **1c**.

Finally, the calculated ECD spectrum at the CAM-B3LYP/6-31++G(d,p) level with PCM in MeOH agreed with the experimental ECD spectrum (Figure 8), allowing an obvious assignment of the absolute structure to be 1*S*,3*S*,6*R*,7*S*,10*R*.

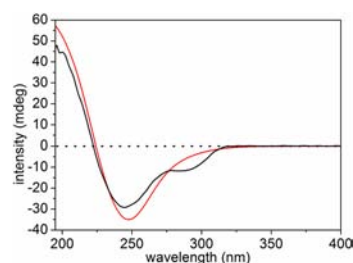


Figure 8. Experimental (black line) and calculated (red line) ECD spectra of **1c** in MeOH.

The molecular orbital (MO) analysis (Figure S35) of the predominant conformer gave us a good understanding of the experimental ECD spectrum. The experimental curve exhibited a negative Cotton effect at 281 nm, which was attributed to the electronic transitions from MO67 to MO70 involving an $n \rightarrow \pi^*$ transition of the ketone group in the cyclobutane unit, and the negative Cotton effect at 249 nm was attributed to the electronic transitions from MO67 to MO68 involving a $\pi \rightarrow \pi^*$ transition of the α,β -unsaturated carboxyl.

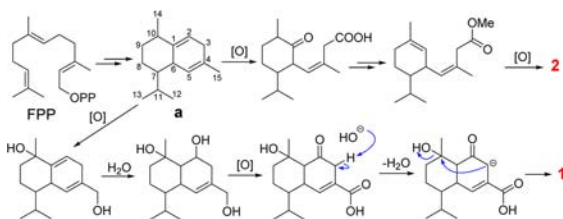
Kadcocinin B (**2**) was assigned to have a molecular formula of $\text{C}_{16}\text{H}_{24}\text{O}_4$ by the HRESIMS at m/z 303.1572 ($[\text{M} + \text{Na}]^+$, calculated as 303.1567), indicating five indices of hydrogen deficiency. Careful examination of the ^1H and ^{13}C NMR spectroscopic data (Tables S2 and S3) disclosed the characteristic of a rare 1,2-*seco*-cadinane sesquiterpenoid. The proposed structure of compound **2** was finally ascertained by the detailed interpretation of the HSQC, ^1H – ^1H COSY, HMBC, and ROESY spectra analyses (Figure S4). In view of the misdiagnosis of gliocladic acid as *5S* and 10*R*,⁹ here we corrected the misrepresentation of gliocladic acid to be *5R* and 10*R*. When the ECD spectrum of compound **2** (Figure S33) was compared to that of gliocladic acid,⁹ the nearly opposite Cotton absorptions at approximately 227 and 260 nm indicated that the absolute configuration of compound **2** was undisputedly 6*S* and 7*S*.

Remarkably, when the crystallography was improbable or impractical, determining the absolute configuration of the cage-

like architecture of kadcocinin A (**1**) creates a significant challenge. To our delight, a quantum-chemical calculation of chemical shifts was a very reliable tool in the structural characterization of complex natural products, and previously, several typical examples have been reported.^{8g,10} Particularly, the structural characterization of **1** was difficult because analysis of 1D and 2D NMR spectroscopic data resulted in three possible structures. Interestingly, these pitfalls can be avoided by utilizing computational methods, especially in conjunction with the scrupulous implementation of state-of-the-art NMR experiments resulting in a final determination of the absolute configuration of **1**. Structurally, **1** belongs to a tricyclo[4.4.0.0^{3,10}]decane scaffold characterized by a special bicyclo[3.1.1]heptane moiety, in which a cyclobutane unit could give rise to a large, long-range spin–spin coupling ($^4J_{1,3} \approx 7$ Hz).

The plausible biosynthetic pathway for compounds **1** and **2** was proposed as follows (Scheme 1). Starting from the farnesyl

Scheme 1. Hypothetical Biogenetic Pathway for Compounds 1 and 2



pyrophosphate (FPP) by the enzymatic cyclization reactions, the key intermediate **a** was generated. Ultimately, the key redox reactions led to **2**, and the vital steps of the Favorskii-like rearrangement led to C-3–C-10 carbon–carbon bond formation, which created **1**.

The cage-like architecture of kadcocinin A (**1**) was of great interest; thus the question of whether **1** was a natural product or artificial product emerged. By the UPLC-MS/MS analyses (Figures S1–S3), **1** could be clearly detected from the total crude extract, suggesting the natural occurrence of **1**.

Compounds **1** and **2** were initially tested for cytotoxicity against HL-60, SMMC-7721, A-549, MCF-7, SW-480, and HeLa human cancer cell lines with the MTS method as previously reported.⁷ Unfortunately, neither compound displayed significant inhibitory effects against those cells with $IC_{50} > 40$ μ M. Additionally, **1** and **2** exhibited weak antifungal effects against *F. oxysporum*, *G. graminis*, and *V. cinnabarium* (Table S1) with MIC_{50} values ranging from 66.4 to 119.9 μ g/mL.

In summary, the research involving the Schisandraceae sesquiterpenoids is limited, and the most representative example of this type was (+)-schisanwilsonene A,¹¹ which was completed by the first enantioselective synthesis. Predictably, the discovery of the cage-like architecture of **1** will provide new insight into the Schisandraceae family. Moreover, it is likely to become an attractive target for synthetic organic chemists in the future.

■ ASSOCIATED CONTENT

Supporting Information

The Supporting Information is available free of charge on the ACS Publications website at DOI: 10.1021/acs.orglett.6b00919.

Experimental details; 1D and 2D NMR, MS, HRESIMS, UV, IR, OR, and CD spectra of **1** and **2**; and computational data for **1** (PDF)

■ AUTHOR INFORMATION

Corresponding Authors

*E-mail: zhangyh@mails.tjmu.edu.cn.

*E-mail: pujianxin@mail.kib.ac.cn.

Author Contributions

[§]Z.-X.H. and Y.-M.S. contributed equally.

Notes

The authors declare no competing financial interest.

■ ACKNOWLEDGMENTS

This project was supported by the National Natural Science Foundation of China (Nos. 81373290 and 21322204) and the NSFC-Joint Foundation of Yunnan Province (U1302223).

■ REFERENCES

- (1) (a) Xiao, W. L.; Li, R. T.; Huang, S. X.; Pu, J. X.; Sun, H. D. *Nat. Prod. Rep.* **2008**, *25*, 871–891. (b) Shi, Y. M.; Xiao, W. L.; Pu, J. X.; Sun, H. D. *Nat. Prod. Rep.* **2015**, *32*, 367–410.
- (2) (a) Pu, J. X.; Xiao, W. L.; Lu, Y.; Li, R. T.; Li, H. M.; Zhang, L.; Huang, S. X.; Li, X.; Zhao, Q. S.; Zheng, Q. T.; Sun, H. D. *Org. Lett.* **2005**, *7*, 5079–5082. (b) Gao, X. M.; Pu, J. X.; Xiao, W. L.; Huang, S. X.; Lou, L. G.; Sun, H. D. *Tetrahedron* **2008**, *64*, 11673–11679.
- (3) (a) Sun, H. D.; Qiu, S. X.; Lin, L. Z.; Wang, Z. Y.; Lin, Z. W.; Pengsuparp, T.; Pezzuto, J. M.; Fong, H. H. S.; Cordell, G. A.; Farnsworth, N. R. *J. Nat. Prod.* **1996**, *59*, 525–527. (b) Luo, X.; Shi, Y. M.; Luo, R. H.; Luo, S. H.; Li, X. N.; Wang, R. R.; Li, S. H.; Zheng, Y. T.; Du, X.; Xiao, W. L.; Pu, J. X.; Sun, H. D. *Org. Lett.* **2012**, *14*, 1286–1289. (c) Liang, C. Q.; Shi, Y. M.; Luo, R. H.; Li, X. Y.; Gao, Z. H.; Li, X. N.; Yang, L. M.; Shang, S. Z.; Li, Y.; Zheng, Y. T.; Zhang, H. B.; Xiao, W. L.; Sun, H. D. *Org. Lett.* **2012**, *14*, 6362–6365.
- (4) Shi, Y. M.; Wang, X. B.; Li, X. N.; Luo, X.; Shen, Z. Y.; Wang, Y. P.; Xiao, W. L.; Sun, H. D. *Org. Lett.* **2013**, *15*, 5068–5071.
- (5) Shi, Y. M.; Yang, J.; Xu, L.; Li, X. N.; Shang, S. Z.; Cao, P.; Xiao, W. L.; Sun, H. D. *Org. Lett.* **2014**, *16*, 1370–1373.
- (6) (a) Goh, S. S.; Baars, H.; Gockel, B.; Anderson, E. A. *Org. Lett.* **2012**, *14*, 6278–6281. (b) Li, J.; Yang, P.; Yao, M.; Deng, J.; Li, A. J. *Am. Chem. Soc.* **2014**, *136*, 16477–16480. (c) Gockel, B.; Goh, S. S.; Puttock, E. J.; Baars, H.; Chaubet, G.; Anderson, E. A. *Org. Lett.* **2014**, *16*, 4480–4483. (d) Wang, L.; Wang, H. T.; Li, Y. H.; Tang, P. P. *Angew. Chem., Int. Ed.* **2015**, *54*, 5732–5735. (e) You, L.; Liang, X. T.; Xu, L. M.; Wang, Y. F.; Zhang, J. J.; Su, Q.; Li, Y. H.; Zhang, B.; Yang, S. L.; Chen, J. H.; Yang, Z. J. *Am. Chem. Soc.* **2015**, *137*, 10120–10123. (f) Goh, S. S.; Chaubet, G.; Gockel, B.; Cordonnier, M. C. A.; Baars, H.; Phillips, A. W.; Anderson, E. A. *Angew. Chem., Int. Ed.* **2015**, *54*, 12618–12621. (g) Wang, Y.; Li, Z. L.; Lv, L. B.; Xie, Z. X. *Org. Lett.* **2016**, *18*, 792–795.
- (7) Hu, Z. X.; Shi, Y. M.; Wang, W. G.; Li, X. N.; Du, X.; Liu, M.; Li, Y.; Xue, Y. B.; Zhang, Y. H.; Pu, J. X.; Sun, H. D. *Org. Lett.* **2015**, *17*, 4616–4619.
- (8) (a) Meinwald, J.; Lewis, A. J. *Am. Chem. Soc.* **1961**, *83*, 2769–2770. (b) Wiberg, K. B.; Lowry, B. R.; Nist, B. J. *J. Am. Chem. Soc.* **1962**, *84*, 1594–1597. (c) Uchio, Y.; Matsuo, A.; Nakayama, M.; Hayashi, S. *Tetrahedron Lett.* **1976**, *17*, 2963–2966. (d) Uchio, Y. *Tetrahedron* **1978**, *34*, 2893–2899. (e) Ognyanov, I.; Todorova, M.; Dimitrov, V.; Ladd, J.; Irngartinger, H.; Kurda, E.; Rodewald, H. *Phytochemistry* **1983**, *22*, 1775–1777. (f) Meinwald, J. *J. Org. Chem.* **2005**, *70*, 4903–4909. (g) Lodewyk, M. W.; Soldi, C.; Jones, P. B.; Olmstead, M. M.; Rita, J.; Shaw, J. T.; Tantillo, D. J. *J. Am. Chem. Soc.* **2012**, *134*, 18550–18553.
- (9) Yan, S.; Li, S.; Wu, W.; Zhao, F.; Bao, L.; Ding, R.; Gao, H.; Wen, H. A.; Song, F.; Liu, H. W. *Chem. Biodiversity* **2011**, *8*, 1689–1700.
- (10) (a) Yang, C. S.; Wang, X. B.; Wang, J. S.; Luo, J. G.; Luo, J.; Kong, L. Y. *Org. Lett.* **2011**, *13*, 3380–3383. (b) Ji, N. Y.; Liu, X. H.; Miao, F. P.; Qiao, M. F. *Org. Lett.* **2013**, *15*, 2327–2329. (c) Shi, Y. M.; Cai, S. L.; Li, X. N.; Liu, M.; Shang, S. Z.; Du, X.; Xiao, W. L.; Pu, J. X.; Sun, H. D. *Org. Lett.* **2016**, *18*, 100–103.
- (11) Gaydou, M.; Miller, R. E.; Delpont, N.; Ceccon, J.; Echavarren, A. M. *Angew. Chem., Int. Ed.* **2013**, *52*, 6396–6399.